—Original Article—

Cell-cycle-dependent Colonization of Mouse Spermatogonial Stem Cells After Transplantation into Seminiferous Tubules

Kei ISHII[1], Mito KANATSU-SHINOHARA[1] and Takashi SHINOHARA[1,2]

[1]*Department of Molecular Genetics, Graduate School of Medicine, Kyoto University, Kyoto 606-8501, Japan*
[2]*CREST, Japan Science and Technology Agency, Kyoto 606-8501, Japan*

Abstract. Spermatogonial stem cells (SSCs) migrate to the niche upon introduction into the seminiferous tubules of the testis of infertile animals. However, only 5–10% of the transplanted cells colonize recipient testes. In this study, we analyzed the impact of cell cycle on spermatogonial transplantation. We used fluorescent ubiquitination-based cell cycle indicator transgenic mice to examine the influence of cell cycle on SSC activity of mouse germline stem (GS) cells, a population of cultured spermatogonia enriched for SSCs. GS cells in the G1 phase are more efficient than those in the S/G2-M phase in colonizing the seminiferous tubules of adult mice. Cells in the G1 phase not only showed higher expression levels of GFRA1, a component of the GDNF self-renewal factor receptor, but also adhered more efficiently to laminin-coated plates. Furthermore, this cell cycle-dependency was not observed when cells were transplanted into immature pup recipients, which do not have the blood-testis barrier (BTB) between Sertoli cells, suggesting that cells in the G1 phase may passage through the BTB more readily than cells in the S/G2-M phase. Thus cell cycle status is an important factor in regulating SSC migration to the niche.
Key words: Cell cycle, Sertoli cells, Spermatogenesis, Stem cells, Transplantation

(J. Reprod. Dev. 60: 37–46, 2014)

Spermatogonial stem cells (SSCs) are closely associated with their microenvironment, which provides self-renewal factors for long-term maintenance. The association between stem cells and their environmental niche is dynamic, as SSCs are capable of migrating into the niche of another animal following microinjection into the adluminal compartment of the seminiferous tubules [1]. The process of migrating into the niche, called homing, involves multiple steps. Transplanted SSCs attach to Sertoli cells, pass through the blood-testis barrier (BTB), which consists of tight junction proteins, and settle onto the basement membrane of the seminiferous tubules [2]. SSCs are then able to undergo self-renewal in the germline niche where glial cell line-derived neurotrophic factor (GDNF), a self-renewal factor for SSCs, is produced [3]. Transplantation assays have shown that there are ~1 to 2×10^3 SSCs in the testis [2, 4]; this corresponds to ~5–10% of the total number of A_{single} (A_s) spermatogonia, which are thought to be SSCs [5, 6]. This difference in the number of morphological and functional SSCs suggests that not all A_s spermatogonia are functionally equivalent and that only a portion of A_s spermatogonia are SSCs.

The condition of the host animal is critical for efficient SSC colonization. Administration of leuprolide, a GnRH analogue, increases SSC colonization in both mice and rats [7, 8]. It is considered that ablation of endogenous germ cells prior to transplantation disrupts the endocrine balance of the testis, which can compromise donor cell colonization. Age of the recipient animal is also important. Transplantation of testis cells into pup testes, which lack a fully formed BTB, increases colonization efficiency by 5- to 10-fold [9]. Recent work in our laboratory showed that expression of tight junction proteins, such as claudins, is necessary for transmigration of SSCs through the BTB [10]. These results suggest that only a small population of spermatogonia is capable of colonizing adult seminiferous tubules and that other subsets are responsible for colonization of pup, but not adult, seminiferous tubules.

Heterogeneity within donor cell populations was also noted in previous transplantation studies. Analysis of donor cell colonization patterns revealed considerable variability in the morphology and length of germ cell colonies [2]. While some colonies are very long, short colonies are also found even after long periods of time. It was suggested that such variation in colony pattern results from differences in the times when individual stem cells initiate division, the ratio of stem cell renewal relative to differentiation divisions in each colony, and the degree of degeneration affecting different colonies. This observation was reminiscent of classic experiments on busulfan-induced spermatogonia regeneration, which showed colonies of various sizes [11], suggesting that A_s spermatogonia have different sensitivities to genotoxic insults. In a similar vein, more recent analyses have identified differences in *Neurog3* expression in undifferentiated spermatogonia, some of which may act as SSCs [12]. It was also reported that GFRA1, a component of the GDNF receptor, is heterogeneously expressed in SSCs [13]. Together, these results suggest that SSCs are not comprised of a biologically pure population. However, the mechanism that underlies SSC heterogeneity has remained unknown due in part to small populations and lack of methods for prospective identification of SSCs.

One of the potential factors that influence donor cell heterogeneity is the cell cycle status. Although its potential involvement in spermatogonial transplantation has been discussed, no data demonstrating such an effect have been reported. Because cell cycle status influences homing of hematopoietic stem cells (HSCs) to the bone marrow niche [14], it is reasonable to speculate that cell cycle status also underlies functional heterogeneity of SSCs. However, this issue has not yet been addressed directly. This is due in part to technical limitations including the small number of A_s spermatogonia and to their relatively slow cell cycle. SSCs proliferate actively only following major cell loss as a result of radiation or chemical exposure [5, 15], making it difficult to obtain sufficient number of cells in each cell cycle phase for functional analysis.

In this study, we approached this problem by using germline stem (GS) cells, a population of cultured spermatogonia with enriched SSC activity. GS cells are derived from postnatal germ cells by culture in GDNF-supplemented medium [16]. Addition of GDNF stimulates active replication of spermatogonial cells, making it possible to obtain a large number of SSCs for molecular and biochemical analyses. To analyze the impact of cell cycle on SSC activity, we derived GS cells from fluorescent ubiquitination-based cell cycle indicator (Fucci) transgenic mice [17]. Fucci technology allows identification of live cells in the G1 and S/G2-M phases by dual-color imaging. The Fucci probe is generated by fusing monomeric Kusabira-Orange 2 (mKO2) and monomeric Azami-Green (mAG) to the ubiquitination domains of human Cdt1 (hCdt1) and human geminin (hGem), respectively. Cdt1 levels are highest in the G1 phase, whereas geminin levels increase during the S phase and decrease during the G1 phase [17]. The activities of these proteins are regulated by ubiquitination, which targets unnecessary proteins for destruction. GS cells were evaluated across all cell cycle phases to determine the effect of cell cycle on cell phenotype and SSC activity on spermatogonial transplantation.

Materials and Methods

Animals and cell culture

Transgenic mouse lines B6.Cg-Tg(Fucci)504Bsi and B6.Cg-Tg(Fucci)596Bsi were purchased from Amalgaam (Tokyo, Japan). For establishing individual Fucci GS cell lines, male Fucci transgenic mice were crossed with wild-type DBA/2 females (Japan SLC, Shizuoka, Japan). Following successful crossing, these mice were then crossed with a transgenic mouse line B6-TgR(ROSA26)26Sor (designated ROSA) female (The Jackson Laboratory, Bar Harbor, ME, USA) in a DBA/2 background to produce triple transgenic mice containing both Fucci transgenes and a LacZ marker. GS cells were established from 5- to 10-day-old pup testes as described previously [16]. Established cells were maintained on plates coated with laminin (20 μg/ml, Sigma, St. Louis, MO, USA) in StemPro-34 SFM (Invitrogen, Carlsbad, CA, USA) as previously described [18]. The culture medium was supplemented with rat GDNF, human FGF2 (both from Peprotech, London, UK), and 1% fetal bovine serum (FBS).

For time-lapse imaging, cells were grown on 35-mm glass-bottom dishes and were analyzed using a computer-assisted fluorescence microscope (FV10i-LIV, Olympus, Tokyo, Japan) equipped with an objective lens (UPLSAPO 60XW, NA=1.2, Olympus), and an excitation LD laser (473 nm and 559 nm)(Olympus). Ten different fields in three dishes were observed, and pictures were taken every 30 min for 72 h.

Laminin-binding assays were carried out as described previously with slight modifications [19]. In brief, plates were coated with laminin (20 μg/ml) for 1 h at room temperature, and GS cells plated at a density of 3×10^5 cells/9.6 cm^2. Following incubation for the indicated period, floating cells were recovered by gently removing the supernatant, and adherent cells were collected by incubation in 0.25% trypsin/1 mM EDTA for 5 min.

Transplantation

For counting of germ cell colonies, ~2×10^3 cells were microinjected into the seminiferous tubules of 4- to 6-week-old WBB6F1-W/W^v (W) mice (Japan SLC). We also transplanted 2×10^2 to 2×10^3 cells into 5- to 10-day-old W pups. For observation of colony pattern formation, ~4×10^5 cells were microinjected into the seminiferous tubules of 4- to 6-week-old W mice. Microinjection was performed through the efferent duct [20]. For all GS cell transplantations, recipient mice were treated with anti-CD4 antibodies to induce tolerance to the donor cells [21]. All animal experimentation protocols were approved by the Institutional Animal Care and Use Committee of Kyoto University.

Analysis of recipient testis

Recipient testes were recovered at indicated time points after transplantation. In experiments using ROSA GS cells, recovered testes were fixed with 4% paraformaldehyde for 2 h at 4 C, and were stained for LacZ activity using X-gal (Wako Pure Chemical Industries, Osaka, Japan) [2]. Donor cell clusters were defined as colonies when they occupied the entire basal surface of the tubule and were at least 0.1 mm in length. For histological evaluation of recipient testes, the testes were fixed with 10% neutral-buffered formalin and processed for paraffin sectioning. Two histological sections were made from each recipient testis with an interval of 12 μm, and were stained with hematoxylin and eosin. For analysis of donor cell colonization patterns, dissociated seminiferous tubules were fixed in 4% paraformaldehyde for 1 h at 4 C before observation under a confocal laser-scanning microscopy (FV1000-D; Olympus).

Immunohistochemistry of testis

Testes were fixed in 4% paraformaldehyde for 2 h at 4 C, embedded in Tissue-Tek OCT compound and processed for cryosectioning. Sections of 10 μm thickness were prepared. Primary and secondary antibodies used are listed in Supplementary Table S1 (on-line only). Hoechst 33342 (Sigma) was used for counterstaining. Sections were observed under a confocal laser-scanning microscope (FV1000-D).

Immunostaining of cultured cells

Single-cell suspensions were concentrated on glass slides by centrifugation using a Cytospin 4 centrifuge (Thermo Electron, Cheshire, UK). For immunostaining, cells were treated with 0.1% Triton-X 100 and 0.1% sodium citrate in phosphate-buffered saline (PBS), and were subsequently fixed in 4% paraformaldehyde for 1 h. Primary and secondary antibodies used are listed in Suppl Table S1.

Real-time polymerase chain reaction (PCR)

Total RNA was recovered using TRIzol following the manufacturer's protocol (Invitrogen). First-strand cDNA was produced using a Verso cDNA Synthesis Kit (Thermo Fisher Scientific, Waltham, MA, USA). PCR conditions were 95 C for 10 min, followed by 40 cycles at 95 C for 15 sec and 60 C for 60 sec. Transcript levels were normalized to that of *Hprt* using a StepOnePlus Real-Time PCR System and *Power* SYBR Green PCR Master Mix (Applied Biosystems, Warrington, UK). PCR was performed using specific primers, which are listed in Supplementary Table S2 (on-line only).

Flow cytometry and cell sorting

Recipient testes were dissociated into single cells using a two-step enzymatic protocol based on collagenase type IV and trypsin digestions, as described previously [20]. GS cells were dissociated using cell dissociation buffer (Invitrogen). Dissociated cells were suspended in PBS containing 1% FBS at a concentration of 1×10^7 cells/ml. Primary and secondary antibodies used are listed in Suppl Table S1. For cell cycle analysis, GS cells were suspended in PBS containing 1% FBS and were incubated in Hoechst 33342 (12.5 μg/ml) for 30 min. All cell sorting and analyses were carried out using the FACSAria III system (BD Biosciences, San Jose, CA, USA).

Statistical analysis

Results are means ± SEM. Significant differences between means for single comparisons were identified using the Student's *t*-test. Multiple comparison analyses were performed using ANOVA followed by Tukey's HSD test.

Results

Expression of Fucci transgenes in undifferentiated spermatogonia

To visualize the cell cycle status of the spermatogonial population of Fucci mice, testes were characterized by immunohistochemistry. Fucci mice expressing Cdt1-KO2 red fluorescence (Fig. 1A), which indicates cells in the G1 phase, were stained with antibodies against CDH1, GFRA1, and ZBTB16. While CDH1 and ZBTB16 are markers of whole undifferentiated spermatogonia population, GFRA1 is more specific and is a marker of the A_s and A_{paired} (A_{pr}) spermatogonia [22]. Approximately 15–25% of cells stained with each of these markers showed Cdt1-KO2 fluorescence (red); no significant difference was observed between markers (Fig. 1B and C). To detect mitotically active cells more specifically, we next carried out similar analyses using Fucci mice expressing Gem-AG green fluorescence (Fig. 1A), which indicates cells in the S/G2-M phase. Gem-AG$^+$ cells were found less often in cells expressing GFRA1 compared with those expressing CDH1 (Fig. 1B and C), suggesting that A_s and A_{pr} spermatogonia divide less frequently than the undifferentiated spermatogonia population as a whole.

Derivation of GS cells from Fucci transgenic mice

To further understand the role of the cell cycle in SSC colonization, we generated Fucci mice expressing both Cdt1-KO2 and Gem-AG transgenes. These mice were then crossed with ROSA mice, which express the LacZ gene ubiquitously to produce triple transgenic
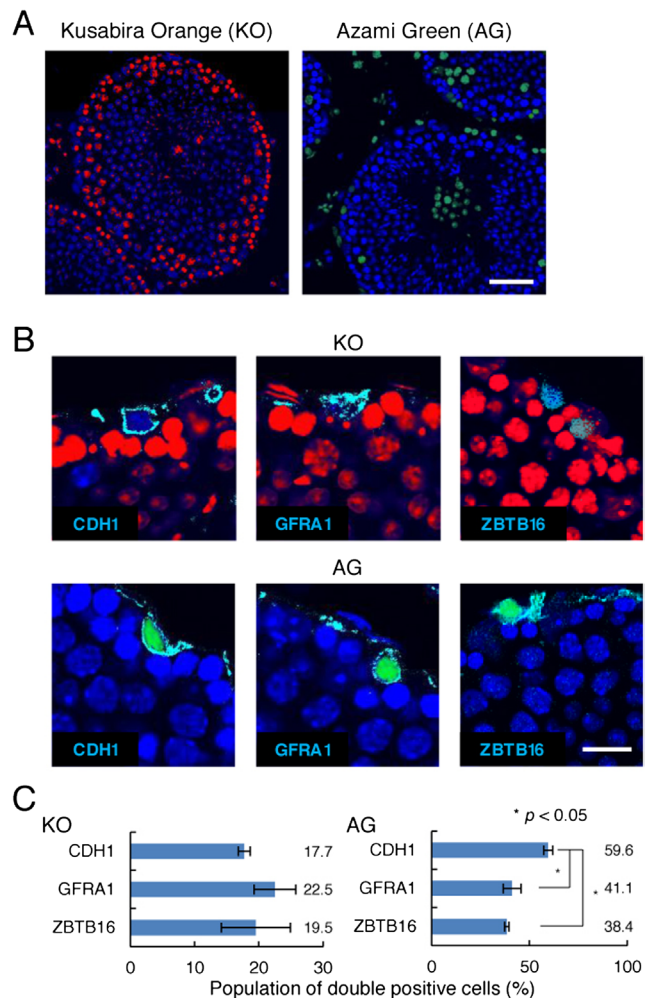

Fig. 1. Expression of Fucci transgenes in the undifferentiated spermatogonia compartment. A: Histological sections of Cdt1-KO2 and Gem-AG transgenic mouse testes. Cdt1-KO2 is expressed predominantly in cells on the basement membrane, while Gem-AG expression is rarely found in the same region. B: Immunostaining of testes using antibodies against markers of undifferentiated spermatogonia. Antibodies against the indicated antigens were used to stain testes of Cdt1-KO2 and Gem-AG transgenic mice. Counterstained with Hoechst 33342 (blue). C: Quantification of cells with undifferentiated spermatogonia marker expression. At least 80 cells with each indicated spermatogonia marker were counted. Bars = 50 μm (A), 20 μm (B).

(Fucci-ROSA) mice. GS cells were then derived from 5- to 10-day-old pups (Fig. 2A).

Consistent with our previous observation using propidium-iodide-based cell cycle analyses [23], GS cells with Cdt1-KO2 fluorescence were observed more frequently than cells expressing Gem-AG florescence. However, no apparent pattern was evident in the distribution of cells with Cdt1-KO2 or Gem-AG fluorescence in these colonies. Flow cytometric analysis showed that cells with Gem-AG fluorescence have greater forward scatter and side scatter values than cells with Cdt1-KO2 fluorescence, suggesting that they
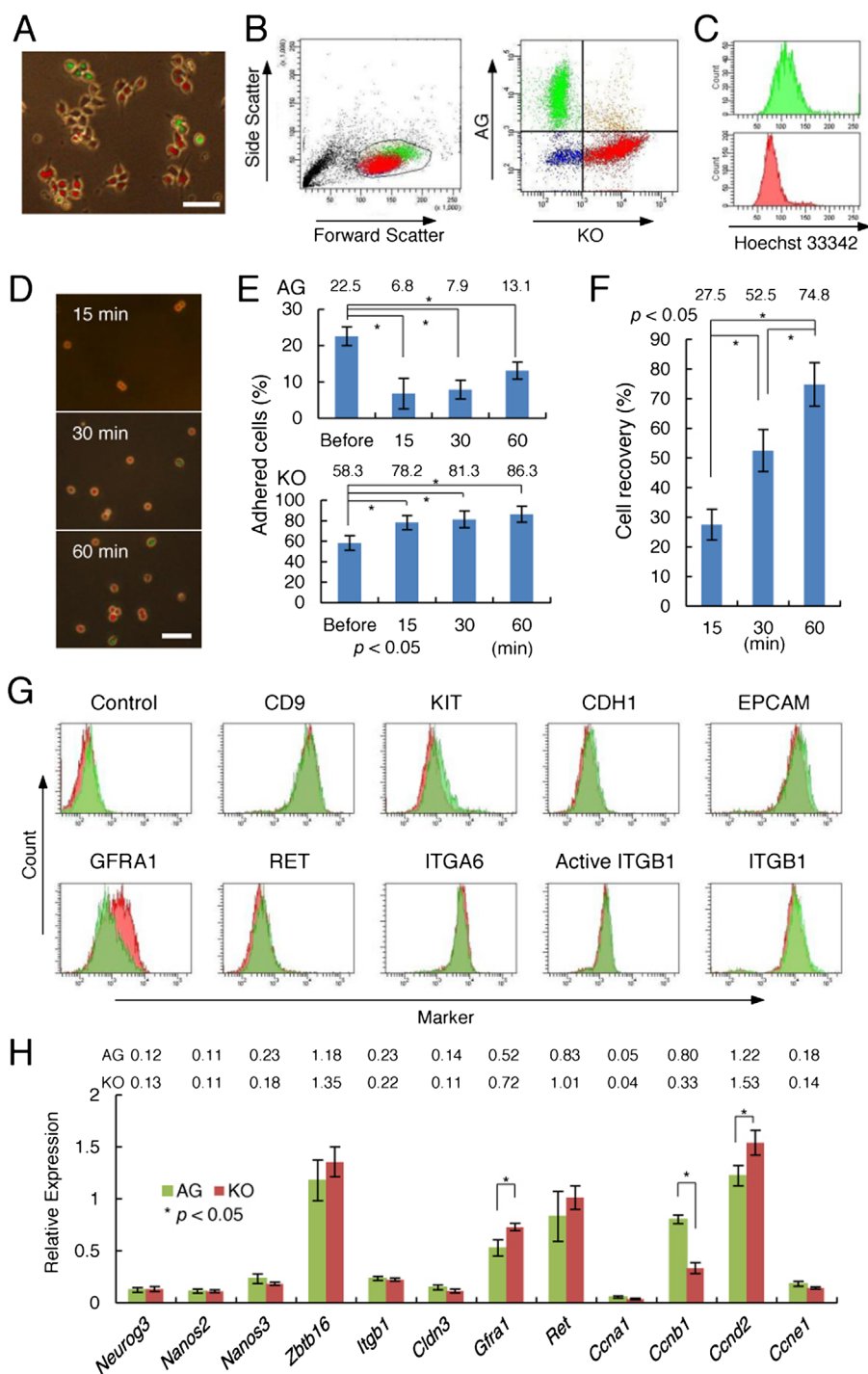
Fig. 2. Derivation of GS cells from Fucci mice. A: Appearance of GS cells derived from a transgenic mouse pup containing both Cdt1-KO2 and Gem-AG transgenes. B: Flow cytometric analysis of Fucci transgene expression in GS cells. C: Flow cytometric analysis of the cell cycle distribution of Fucci-ROSA GS cells using Hoechst 33342. GS cells were stained with Hoechst 33342 for analysis of DNA content. D: Relative increase in adhesion of Cdt1-KO2$^+$ GS cells to laminin-coated plates. Logarithmically growing GS cells were dissociated by trypsin and incubated on laminin-coated plates for the indicated time. E: Quantification of cells with Cdt1-KO2 or Gem-AG fluorescence that attached to laminin. At least 112 cells in 15 random fields were counted in four experiments. Cells were incubated on laminin-coated plates for the indicated time, and were recovered with trypsin for cell counting. The proportion of cells with Cdt1-KO2 or Gem-AG fluorescence is indicated. The results were compared with logarithmically growing cells (Before). F: Recovery of GS cells from laminin-coated plates (n = 4). The cells were incubated for the indicated time, and total adherent cell number was determined after collecting attached cells with trypsin. G: Flow cytometric analysis of cell surface marker expression. GS cells with Cdt1-KO2 or Gem-AG fluorescence were gated and analyzed for the expression of surface antigens. H: Real-time PCR analysis of GS cells. Fucci-ROSA GS cells were sorted according to their transgene expression patterns, and mRNA from each fraction was collected for real-time PCR (n = 3). Bar = 20 μm (A, D).

are larger and have more complex structures than those in the G1 phase (Fig. 2B). DNA quantification using Hoechst 33342 showed that cells with Cdt1-KO2$^+$ fluorescence, which comprised ~60% of the total cell population, were in the G1 phase (2n), while cells with Gem-AG$^+$ florescence, comprising ~20% of the total cells, were found to be in the S/G2-M phase (Fig. 2C). We also used time-lapse imaging to monitor live cells to evaluate cell cycle length. We cultured the cells for 72 h and observed changes in fluorescence levels (Supplementary Fig. S1: on-line only). Although GS cells migrated dynamically during this period, a total of 23 cells were randomly recorded for analysis (Table 1). The average cell cycle length was 38.3 h, and Cdt1-KO2 or Gem-AG fluorescence was observed for 24.7 or 12.2 h, respectively.

During passage of GS cells on laminin-coated plates, we noted that Cdt1-KO2$^+$ cells adhered more efficiently than Gem-AG$^+$ cells (Fig. 2D), suggesting that cells in the G1 phase have a greater ability to attach. To determine the kinetics of cell adhesion, Petri dishes were coated with laminin, and GS cells were plated and incubated for 15, 30, and 60 min. Analyses under UV light showed that, while the proportion of adherent Gem-AG$^+$ cells was diminished by replating, Cdt1-KO2$^+$ cells bound more efficiently to laminin as soon as 15 min after plating, which increased gradually up to 60 min (Fig. 2E). The recovery of cells attached to laminin-coated plates increased in a time-dependent manner (Fig. 2F). These results suggest that the adhesiveness of SSCs is influenced by cell cycle status.

Phenotypes of GS cells in the various cell cycle phases

Using flow cytometry, we first determined whether the cell cycle has any impact on spermatogonia marker expression, including ITGB1 and ITGA6, which comprise a laminin receptor involved in SSC homing [19]. Dissociated GS cells were gated according to the transgene expression patterns, and expression levels of spermatogonia markers were examined (Fig. 2G). We used antibodies against several known spermatogonia markers, including ITGB1, ITGA6, CDH1, EPCAM, CD9, RET, KIT, and GFRA1. Contrary to our expectation, we were unable to find significant differences in the expression levels of ITGB1 and ITGA6. No difference in ITGB1 expression was found even by immunostaining with 9EG7, a monoclonal antibody to a conformation-specific epitope exposed only on activated ITGB1. Although we did not observe significant changes in the expression of most of the other spermatogonia markers, GFRA1, a component of GDNF self-renewal factor receptor, was more strongly expressed in Cdt1-KO2$^+$cells. In contrast, expression of RET, another component of the GDNF receptor, was not significantly affected by cell cycle stage.

Using fluorescence-activated cell sorting (FACS), we next separated GS cells in various cell cycle phases, and determined differences in gene expression patterns by real-time PCR (Fig. 2H). As expected from the cell cycle-based separation, the *Ccnb1* gene was expressed more strongly in Gem-AG$^+$ cells. In contrast, *Ccnd2*, a gene involved in GS cell proliferation and expressed throughout the cell cycle [24, 25], was expressed more strongly in Cdt1-KO2$^+$ cells. No significant difference was found in the levels of *Ccna1* and *Ccne1*. Spermatogonial transcription factors and adhesion molecules were expressed at comparable levels in Cdt1-KO2$^+$ and Gem-AG$^+$ cells. However, we did observe a significant increase in the expression of *Gfra1* in Cdt1-KO2$^+$ cells, consistent with the flow cytometry results.

Table 1. Time lapse analysis of GS cells

Cell type	Time (h) (n=23)
KO$^-$AG$^-$ (late M~early G1)	2.5 ± 1.3
KO$^-$AG$^+$ (middle S~late M)	11.1 ± 1.4
KO$^+$AG$^-$ (early G1~late G1)	23.6 ± 4.7
KO$^+$AG$^+$ (early S)	1.1 ± 0.1
Total	38.3 ± 6.8

Values are mean ± SEM. Ten different fields in three dishes were analyzed.

Although *Ret* was also expressed more strongly in Cdt1-KO2$^+$ cells, the difference was not statistically significant. Together, these results suggest that GS cells in the G1 phase are more sensitive to cytokine stimulation than those in other cell cycle phases.

Pattern of cell cycle distribution in germ cell colonies after transplantation

To examine the relationship between the cell cycle and colony formation, we transplanted Fucci-ROSA GS cells into congenitally infertile W mice, which do not have endogenous spermatogenesis. Some of the recipient testes were examined at increasing time intervals under UV light. Recipient testes were dissociated at 1 day, 2 weeks, 1 month, and 2 months following transplantation, and analyzed by flow cytometry. Whole mount analysis of the seminiferous tubules under confocal microscopy showed that, immediately after transplantation, single donor cells were distributed randomly in the seminiferous tubules. At this stage, the majority of donor cells existed as single cells (Fig. 3A), and cells expressing Gem-AG$^+$ fluorescence could be readily detected. Two weeks after transplantation, donor cells were significantly decreased, but distinct clusters of germ cells were evident on the basement membrane. We found not only doublets but also chains of spermatogonia on the basal membrane (Fig. 3B). Evaluation of donor cell fluorescence by flow cytometry showed that an increased number of cells expressed Cdt1-KO2$^+$ at this stage (Fig. 3C). By 1 month, donor cells established two-dimensional monolayer colonies on the basement membrane, which were comprised predominantly of Cdt1-KO2$^+$ cells. The proportion of Gem-AG$^+$ cells was decreased relative to Cdt1-KO2$^+$ cells at this stage (Fig. 3D). By two months, when donor cells produce round and elongated spermatids, cells expressing Gem-AG fluorescence were more frequently found along colony edges, whereas cells in the center of the colonies were expressing primarily Cdt1-KO2, suggesting that germ cell proliferation is concentrated at the extremities (Fig. 3E and Table 2).

Flow cytometric analyses of the recipient testes showed that the proportion of cells expressing Cdt1-KO2 fluorescence was higher at 2 months than at 1 month after transplantation. Cells at this stage showed larger forward scatter values, which reflects development of meiotic cells from the transplanted donor cells [26]. Immunostaining showed that transplantation influences undifferentiated marker expression (Fig. 3F and G). While GFRA1$^+$ or ZBTB16$^+$ cells were fewer than CDH1$^+$ cells before transplantation in Gem-AG$^+$ cells (Fig. 1C), no such difference was found after transplantation. This result suggests that GFRA1 expression is sensitive to growth stimulation, which is consistent with previous observations [27].
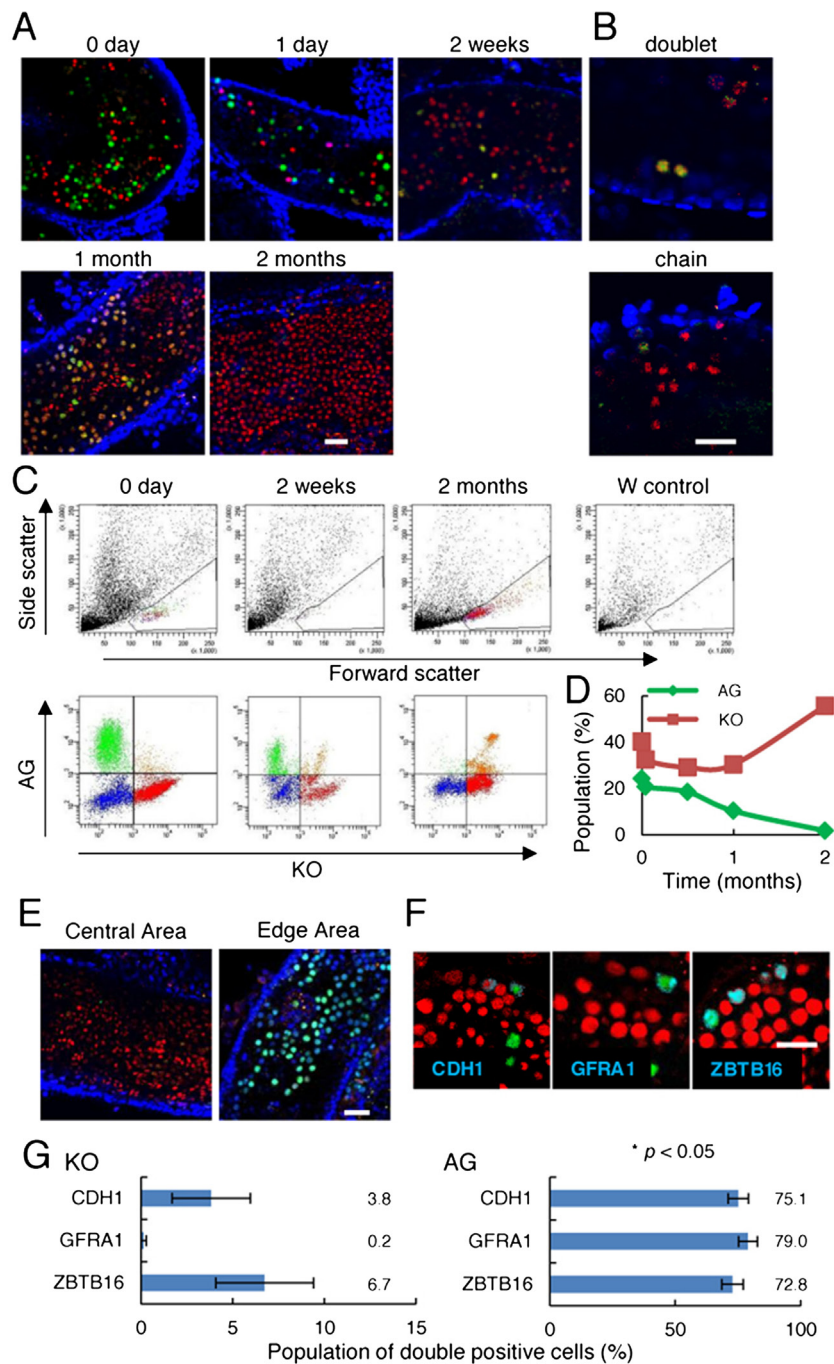
Fig. 3. Colonization of recipient mouse seminiferous tubules by Fucci-ROSA GS cells at intervals up to 2 months after transplantation. A: Whole mount appearance of seminiferous tubules that received transplantation of Fucci-ROSA GS cells. Seminiferous tubules were collected at the indicated time and were analyzed under UV light. Note the decrease in the proportion of cells with Gem-AG fluorescence. B: Doublet (top) and chain (bottom) of spermatogonia on the basement membrane at 2 weeks after transplantation. C: Flow cytometric analysis of recipient testes. Recipient testes were dissociated into single cells, and expression patterns of the Fucci transgenes were compared. Forward scatter and side scatter profiles change as donor cells differentiate into haploid cells. D: Quantification of cells with Cdt1-KO2^{+} or Gem-AG[+] fluorescence by flow cytometry. The proportions of cells expressing Cdt1-KO2 or Gem-AG fluorescence were plotted using data from flow cytometric analysis at the indicated time points. E: Fucci transgene expression in the central and edge regions of germ cell colonies 2 months after transplantation. F: Immunostaining of recipient testes 2 months after transplantation. Antibodies against indicated antigens were used to stain testes of Cdt1-KO2 and Gem-AG transgenic mice. Counterstained with Hoechst 33342 (blue). G: Quantification of cells expressing undifferentiated spermatogonia markers. At least 178 cells with each indicated spermatogonia marker were counted. Bar = 20 μm (A, B, E, F).

Table 2. Distribution of fluorescent cell type in germ cell colonies

Cell type	Central Area (n = 7)	Edge Area (n = 11)
KO⁻ AG⁻ (late M~early G1)	2.3 ± 0.3	8.0 ± 0.7
KO⁻ AG⁺ (middle S~late M)	10.0 ± 1.0	52.4 ± 3.0
KO⁺ AG⁻ (early G1~late G1)	84.6 ± 1.3	33.1 ± 3.2
KO⁺ AG⁺ (early S)	3.1 ± 0.6	6.5 ± 0.7

Values are mean ± SEM. Colonies were analyzed 2 months after transplantation. A total of 3,681 and 4,629 cells (0.4 mm tubule length) were counted for central and edge areas, respectively. The central area was more than 1.0 mm away from the colony edge.

Functional analysis of SSC activity by spermatogonial transplantation

We finally examined the SSC activity of GS cells among the various cell cycle phases. Because SSCs are not prospectively identified by their morphology, it was necessary to examine their identity by functional assay; only 1–2% of GS cells are capable of forming germ cell colonies upon transplantation into seminiferous tubules [18]. We subfractionated Fucci-ROSA GS cells according to the cell cycle status, and equal numbers of cells were microinjected into the seminiferous tubules of W mice. Two months after transplantation, recipient testes were collected and stained for LacZ activity of the donor cells (Fig. 4A). The numbers of colonies generated by Cdt1-KO2⁻/Gem-AG⁻, Cdt1-KO2⁻/Gem-AG⁺, Cdt1-KO2⁺/Gem-AG⁻, Cdt1-KO2⁺/Gem-AG⁺, and unfractionated cells were 12.5, 50.0, 275.0, 0, and 125.0 per 10^5 transplanted cells, respectively. The value was significantly greater for Cdt1-KO2⁺/Gem-AG⁻ cells (Fig. 4B). Cdt1-KO2⁻/Gem-AG⁺ or Cdt1-KO2⁺/Gem-AG⁺ cells produced fewer colonies than unfractionated control GS cells, and these differences were also statistically significant. Histological analysis of recipient testes showed normal spermatogenesis from transplanted Cdt1-KO2⁺/Gem-AG⁻ cells (Fig. 4C), indicating that GS cells in the G1 phase are significantly enriched for SSCs.

To gain insight into the mechanism of cell-cycle-dependent colonization, we used immature W pups; these mice lack the BTB between Sertoli cells. Our previous studies showed that the absence of a fully formed BTB increases the colonization efficiency of SSCs [9]. Equal numbers of GS cells in each cell cycle phase were transplanted into 5- to 10-day old pups. Recipient testes were analyzed 2 months after transplantation, and donor cell-derived colonies were enumerated (Fig. 5A). Consistent with previous studies, the number of colonies was increased compared with adult recipients; the number of colonies generated by Cdt1-KO2⁻/Gem-AG⁻, Cdt1-KO2⁻/Gem-AG⁺, Cdt1-KO2⁺/Gem-AG⁻, Cdt1-KO2⁺/Gem-AG⁺, and unfractionated cells were 77.5, 363.6, 836.1, 656.3, and 382.1 per 10^5 transplanted cells, respectively (Fig. 5B). Although Cdt1-KO2⁺/Gem-AG⁻ cells produced a greater number of colonies, no significant differences were found between donors in each cell cycle phase. Moreover, no enrichment of SSCs was found for cells in any cell cycle phase.

Because activation of RAC1 is involved in transmigration through the BTB [10], we carried out immunostaining of GS cells using antibodies against activated RAC1. We also analyzed the expression of CLDN3, CLDN7, and CLDN8, whose expression in GS cells is regulated by *Rac1*. No significant differences in expression levels
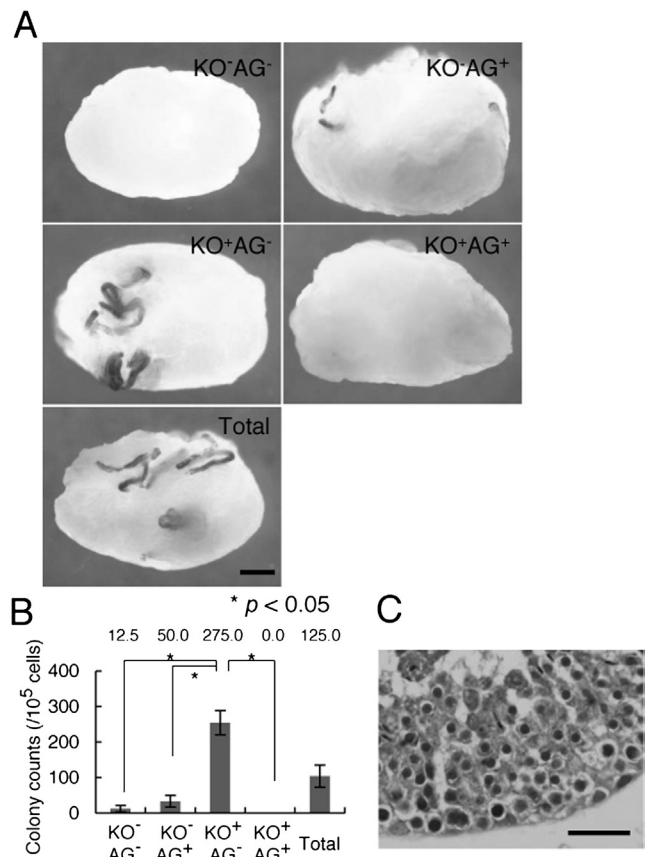
Fig. 4. Functional analysis of SSC activity by spermatogonial transplantation into adult recipients. A: Macroscopic appearance of recipient testes following transplantation of Fucci-ROSA GS cells after cell sorting. Equal numbers of cells were transplanted, and the testes were recovered for LacZ staining 2 months after transplantation. Individual blue tubules indicate colonies of spermatogenesis arising from donor stem cells. B: Colony number. Results of three transplantation experiments using 12 recipient testes. C: Histological appearance of a recipient testis that received transplantation of Cdt1-KO2⁺/Gem-AG⁻ cells. Bars = 1 mm (A), 20 μm (C).

were found, with greater than 99% of all cells expressing each of the four molecules regardless of cell cycle status (Fig. 5C).

Discussion

Because stem cells are defined by their ability to self-renew, the discrepancy between the A_s population and SSC numbers has been an enigma since early transplantation studies [2]. Studies in HSCs have shown that long-term engraftment potential resides predominantly in the G0 phase [14]. Although the mechanism of the stem cell reconstitution machinery may differ between these two self-renewing systems, this effect on HSC colonization suggested that SSC colonization is also influenced by the cell cycle. Thus we assessed the impact of cell cycle stage on SSC homing. The cell cycle was shown to influence not only morphology and adhesive
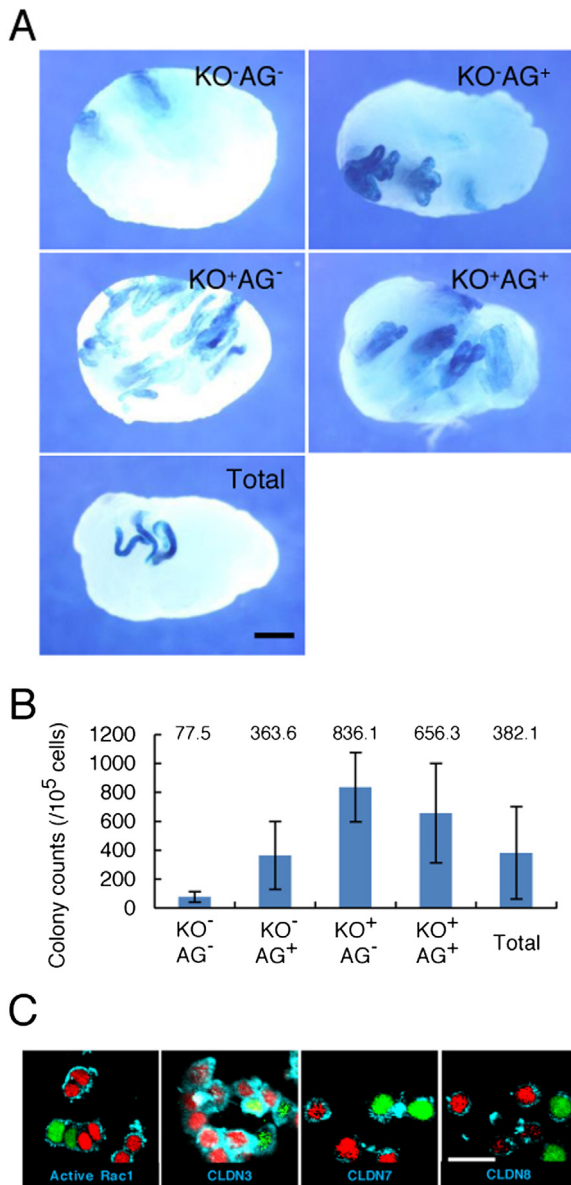
Fig. 5. Functional analysis of SSC activity by spermatogonial transplantation into pup recipients. A: Macroscopic appearance of recipient testes following transplantation of Fucci-ROSA GS cells after cell sorting. Equal numbers of cells were transplanted, and the testes were recovered for LacZ staining 2 months after transplantation. Individual blue tubules indicate colonies of spermatogenesis arising from donor stem cells. B: Colony number. Results of seven transplantation experiments involving at least 11 recipient testes. C: Immunostaining of GS cells using antibodies against activated RAC1, CLDN3, CLDN7, and CLDN8. Logarithmically growing GS cells were centrifuged by cytospin and stained with the indicated antibodies. Bars = 1 mm (A), 20 μm (C).

Several previous studies have suggested a role for the cell cycle in SSC activity. One study showed that SSCs are most sensitive to X-rays during quiescence and most resistant during active proliferation [28]. In contrast, no sensitization was found for differentiating spermatogonia, which do not go through a G0 phase. The impact of the cell cycle on SSCs has also been suggested by more recent studies. SSCs were stained with Hoechst 33342, and cells with a side population (SP) phenotype were isolated using flow cytometry; SP cells, which are enriched for cells in the G1 phase, were shown to have a higher SSC activity than those in the non-SP population [29–31]. However, the SP phenotype is based primarily on transporter activity, and is therefore not a true measure of cell cycle status [32]. In fact, studies of HSCs suggest that the SP cell population also contains cells in the S/G2-M phases [33]. Moreover, Hoechst 33342 exhibits toxicity to SSCs [34], which makes interpretations of these results more complicated. In this context, our use of Fucci reporter technology is advantageous, as it enables visualization of cells in each of the cell cycle phases based upon the activity of the cell cycle machinery. Our use of Fucci mice allowed us to analyze changes in SSC activity and the cell cycle status of germ cell colony development.

We found that GS cells expressing Cdt1-KO2 fluorescence were significantly enriched for SSCs. One factor that may contribute to higher SSC activity is stronger adhesiveness to the extracellular matrix. Our analyses clearly showed that cells in the G1 phase are more efficient in attaching to laminin-coated plates, while those in the S/G2-M are less adhesive. Because SSC activity was stronger in the G1 phase, this may explain why we were able to enrich SSCs by laminin selection in previous studies [35, 36]. This finding marks a distinction between SSCs and hematopoietic progenitors; CD34^{+} progenitor cells in the S/G2-M phase express more ITGA4 and adhere to the stromal cell monolayer more efficiently than cells in the G0/G1 phase [37]. In SSCs, adhesion to laminin is mediated by ITGB1 and ITGA6, and GS cells lose their ability to bind laminin following deletion of ITGB1 [19]. Because ITBG1 expression was not influenced by the cell cycle phase, intracellular regulation of ITGB1 affinity may modify SSC adhesiveness. A search of the literature, in combination with database mining, has defined the integrin "adhesome", which contains ~90 molecules [38, 39]. It is possible that some of these molecules are influenced by the cell cycle and modify adhesiveness. We also do not know about the regulation of ITGA6, which is involved in the adhesion to laminin. A previous study showed that the cytoplasmic domain of the integrin alpha component also modulates integrin function [40].

Another factor that may contribute to higher SSC activity in Cdt1-KO2^{+} cells is the higher expression levels of GFRA1. GDNF is one of the chemotactic factors for SSCs [41, 42]. Inhibition of GDNF signaling through expression of a dominant negative RET receptor significantly impaired GS cell colonization *in vivo*. Higher expression of GFRA1 in Cdt1-hKO2^{+} cells suggests that cells in the G1 phase are more sensitive to GDNF signaling, leading to increased migration towards the niche, thereby generating more colonies. These attributes of SSCs in the G1 phase likely confer advantages compared with other cell cycle phases.

We noted dynamic changes in Fucci fluorescence during transplantation-induced regeneration. While a significant propor-

properties but also DNA repair and marker expression, including those of stem cells. The cell cycle phase may therefore explain the heterogeneity of the A$_s$ population.

tion of cells were in the S/G2-M phase during the early phase of colonization, cells in the G1 phase predominated at later time points when differentiation took place. Our use of Fucci transgenic mouse has allowed us to examine the changes in cell proliferation profile in transplantation-induced regeneration. The gradual increase in the proportion of Cdt1-KO2$^+$/Gem-AG$^-$ cells in developing colonies is consistent with our previous observations regarding SSC doubling time during busulfan-induced regeneration [4]. While SSCs doubled every 6.3 days between 3 and 15 days after busulfan injection, the doubling time increased to 33.9 days between 42 and 70 days. Although we were not able to examine the cell cycle status of SSCs by serial transplantation due to limited cell recovery, the current results strengthen the notion that SSCs have a higher probability of self-renewal immediately after cell loss or transplantation but that differentiation, which occurs at later time points, is accompanied by a decrease in the proportion of rapidly dividing cells.

The distribution of Cdt1-KO2$^+$ and Gem-AG$^+$ cells was not random in established colonies; while Cdt1-KO2$^+$ cells were found more frequently in the center of the colony, Gem-AG$^+$ cells were at the colony edge. GDNF, an SSC self-renewal factor, may be involved in this unequal proliferation pattern. GDNF is expressed at higher levels in germ cell-depleted testes [43]. Given its positive effect on SSC self-renewal, cells at the colony edges may be exposed to higher concentrations of GDNF and proliferate more vigorously, whereas GDNF levels are lower in the middle of the colony where germ cell density is higher. Indeed, cell clumps with high GFRA1 expression, which predominate during early colonization, are preferentially found at the colony edge [44].

Differentiating germ cells can also exert negative influences on growth, including inhibition of undifferentiated spermatogonia proliferation [45]. Adluminal germ cell differentiation occurs in the middle of colonies after they reach a size > 1 mm [2]. During stage III of the epithelium in the normal seminiferous tubule, proliferation is inhibited by the differentiating spermatogonia by way of a negative feedback system. Moreover, spermatogonial degeneration is more marked in animals with a large number of A$_1$ spermatogonia [46]. Such feedback regulation may begin at the colony center and facilitate establishment of recognizable spermatogenic stages, which are observed 2 to 3 months after transplantation [47]. It is possible that germ cells at the colony edge are not subject to negative regulatory mechanisms, and are exposed to high concentrations of GDNF, allowing more active proliferation through induction of GFRA1 expression.

Although we identified a marked impact of the cell cycle on transplantation efficiency in adult testes, its effect was attenuated in pup testes. Because pup testes lack the BTB, we hypothesized that molecules involved in transmigration of SSCs through the BTB may influence cell cycle-dependent colonization. However, no significant changes in the expression patterns of activated RAC1 and several claudins were observed in any cell cycle phases, suggesting that expression and/or regulation of other tight junction proteins may be altered by the cell cycle. We also speculate that differences in colonization pattern and efficiency in pup testes may be due to differences in the cytokine environment. A recent study showed that several chemokines, such as CCL9, CXCL5, and CCL12, are expressed in pup testes and that spermatogonia expressing the CCR1 receptor are attracted to CCL9 [48]. As ETV5 regulates CCL9 expression and ETV5 deficiency results in cessation of spermatogenesis in adult, but not pup, testes [49], pup testes could be exposed to a different cytokine environment, which might have obscured the impact of the cell cycle in pups. These hypotheses should be tested in future experiments.

The Fucci expression system allowed us to assess the impact of the cell cycle on SSC colonization. Isolation and transplantation of cells in each of the cell cycle phases revealed greater SSC potential in GS cells during the G1 phase. This approach can be used to analyze the role of the cell cycle phase in stem cells of other self-renewing tissues. The technique will also facilitate understanding of the impact of candidate genes that influence spermatogonia cell cycle and lineage commitment. Although extension of this technique to SSCs *in vivo* is complicated by their relatively low frequency and lack of SSC-specific markers, such analyses will increase our knowledge of the heterogeneity of spermatogonia and its regulation by the cellular environment.

Acknowledgments

References

1. **Brinster RL, Zimmermann JW.** Spermatogenesis following male germ-cell transplantation. *Proc Natl Acad Sci USA* 1994; **91**: 11298–11302. [Medline] [CrossRef]
2. **Nagano M, Avarbock MR, Brinster RL.** Pattern and kinetics of mouse donor spermatogonial stem cell colonization in recipient testes. *Biol Reprod* 1999; **60**: 1429–1436. [Medline] [CrossRef]
3. **Meng X, Lindahl M, Hyvönen ME, Parvinen M, de Rooij DG, Hess MW, Raatikainen-Ahokas A, Sainio K, Rauvala H, Lakso M, Pichel JG, Westphal H, Saarma M, Sariola H.** Regulation of cell fate decision of undifferentiated spermatogonia by GDNF. *Science* 2000; **287**: 1489–1493. [Medline] [CrossRef]
4. **Kanatsu-Shinohara M, Toyokuni S, Morimoto T, Matsui S, Honjo T, Shinohara T.** Functional assessment of self-renewal activity of male germline stem cells following cytotoxic damage and serial transplantation. *Biol Reprod* 2003; **68**: 1801–1807. [Medline] [CrossRef]
5. **Meistrich ML, van Beek MEAB.** Spermatogonial stem cells. In: Desjardins CC, Ewing LL (eds.), Cell and Molecular Biology of the Testis. New York: Oxford University Press; 1993: 266–295.
6. **Tegelenbosch RAJ, de Rooij DG.** A quantitative study of spermatogonial multiplication and stem cell renewal in the C3H/101 F1 hybrid mouse. *Mutation Res* 1993; **290**: 193–200. [Medline] [CrossRef]
7. **Ogawa T, Dobrinski I, Avarbock MR, Brinster RL.** Leuprolide, a gonadotropin-releasing hormone agonist, enhances colonization after spermatogonial transplantation into mouse testes. *Tissue Cell* 1998; **30**: 583–588. [Medline] [CrossRef]
8. **Ogawa T, Dobrinski I, Brinster RL.** Recipient preparation is critical for spermatogonial transplantation in the rat. *Tissue Cell* 1999; **31**: 461–472. [Medline] [CrossRef]
9. **Shinohara T, Orwig KE, Avarbock MR, Brinster RL.** Remodeling of the postnatal mouse testis is accompanied by dramatic changes in stem cell number and niche accessibility. *Proc Natl Acad Sci USA* 2001; **98**: 6186–6191. [Medline] [CrossRef]
10. **Takashima S, Kanatsu-Shinohara M, Tanaka T, Takehashi M, Morimoto H, Shinohara T.** Rac mediates mouse spermatogonial stem cell homing to germline niches by regulating transmigration through the blood-testis barrier. *Cell Stem Cell* 2011; **9**: 463–475. [Medline] [CrossRef]
11. **van Keulen CJG, de Rooij DG.** Spermatogenetic clones developing from repopulating stem cells surviving a high dose of an alkylating agent. I. First 15 days after injury. *Cell Tissue Kinet* 1975; **8**: 543–551. [Medline]
12. **Yoshida S, Sukeno M, Nabeshima Y.** A vasculature-associated niche for undifferentiated spermatogonia in the mouse testis. *Science* 2007; **317**: 1722–1726. [Medline] [CrossRef]

13. **Grisanti L, Falciatori I, Grasso M, Dovere L, Fera S, Muciaccia B, Fuso A, Berno V, Boitani C, Stefanini M, Vicini E.** Identification of spermatogonial stem cell subsets by morphological analysis and prospective isolation. *Stem Cells* 2009; **27**: 3043–3052. [Medline]

14. **Passegué E, Wagers AJ, Giuriato S, Anderson WC, Weissman IL.** Global analysis of proliferation and cell cycle gene expression in the regulation of hematopoietic stem and progenitor cell fates. *J Exp Med* 2005; **202**: 1599–1611. [Medline] [CrossRef]

15. **de Rooij DG, Russell LD.** All you wanted to know about spermatogonia but were afraid to ask. *J Androl* 2000; **21**: 776–798. [Medline]

16. **Kanatsu-Shinohara M, Ogonuki N, Inoue K, Miki H, Ogura A, Toyokuni S, Shinohara T.** Long-term proliferation in culture and germline transmission of mouse male germline stem cells. *Biol Reprod* 2003; **69**: 612–616. [Medline] [CrossRef]

17. **Sakaue-Sawano A, Kurokawa H, Morimura T, Hanyu A, Hama H, Osawa H, Kashiwagi S, Fukami K, Miyata T, Miyoshi H, Imamura T, Ogawa M, Masai H, Miyawaki A.** Visualizing spatiotemporal dynamics of multicellular cell-cycle progression. *Cell* 2008; **132**: 487–498. [Medline] [CrossRef]

18. **Kanatsu-Shinohara M, Miki H, Inoue K, Ogonuki N, Toyokuni S, Ogura A, Shinohara T.** Long-term culture of mouse male germline stem cells under serum- or feeder-free conditions. *Biol Reprod* 2005; **72**: 985–991. [Medline] [CrossRef]

19. **Kanatsu-Shinohara M, Takehashi M, Takashima S, Lee J, Morimoto H, Chuma S, Raducanu A, Nakatsuji N, Fässler R, Shinohara T.** Homing of mouse spermatogonial stem cells to germline niche depends on β1-integrin. *Cell Stem Cell* 2008; **3**: 533–542. [Medline] [CrossRef]

20. **Ogawa T, Aréchaga JM, Avarbock MR, Brinster RL.** Transplantation of testis germinal cells into mouse seminiferous tubules. *Int J Dev Biol* 1997; **41**: 111–122. [Medline]

21. **Kanatsu-Shinohara M, Ogonuki N, Inoue K, Ogura A, Toyokuni S, Honjo T, Shinohara T.** Allogeneic offspring produced by male germ line stem cell transplantation into infertile mouse testis. *Biol Reprod* 2003; **68**: 167–173. [Medline] [CrossRef]

22. **Nakagawa T, Sharma M, Nabeshima Y, Braun RE, Yoshida S.** Functional hierarchy and reversibility within the murine spermatogenic stem cell compartment. *Science* 2010; **328**: 62–67. [Medline] [CrossRef]

23. **Lee J, Kanatsu-Shinohara M, Inoue K, Ogonuki N, Miki H, Toyokuni S, Kimura T, Nakano T, Ogura A, Shinohara T.** Akt mediates self-renewal division of mouse spermatogonial stem cells. *Development* 2007; **134**: 1853–1859. [Medline] [CrossRef]

24. **Lee J, Kanatsu-Shinohara M, Morimoto H, Kazuki Y, Takashima S, Oshimura M, Toyokuni S, Shinohara T.** Genetic reconstruction of mouse spermatogonial stem cell self-renewal *in vitro* by Ras-cyclin D2 activation. *Cell Stem Cell* 2009; **5**: 76–86. [Medline] [CrossRef]

25. **Sherr CJ.** Cancer cell cycles. *Science* 1996; **274**: 1672–1677. [Medline] [CrossRef]

26. **Malkov M, Fisher Y, Don J.** Developmental schedule of the postnatal rat testis determined by flow cytometry. *Biol Reprod* 1998; **59**: 84–92. [Medline] [CrossRef]

27. **Morimoto H, Kanatsu-Shinohara M, Takashima S, Chuma S, Nakatsuji N, Takehashi M, Shinohara T.** Phenotypic plasticity of mouse spermatogonial stem cells. *PLoS One* 2009; **4**: e7909. [Medline] [CrossRef]

28. **van der Meer Y, Huiskamp R, Davids JA, van der Tweel I, de Rooij DG.** The sensitivity of quiescent and proliferating mouse spermatogonial stem cells to X irradiation. *Radiat Res* 1992; **130**: 289–295. [Medline] [CrossRef]

29. **Falciatori I, Borsellino G, Haliassos N, Boitani C, Corallini S, Battistini L, Bernardi G, Stefanini M, Vicini E.** Identification and enrichment of spermatogonial stem cells displaying side-population phenotype in immature mouse testis. *FASEB J* 2004; **18**: 376–378. [Medline]

30. **Lassalle B, Bastos H, Louis JP, Riou L, Testart J, Dutrillaux B, Fouchet P, Allemand I.** 'Side population' cells in adult mouse testis express Bcrp1 gene and are enriched in spermatogonia and germinal stem cells. *Development* 2004; **131**: 479–487. [Medline] [CrossRef]

31. **Barroca V, Lassalle B, Coureuil M, Louis JP, Le Page F, Testart J, Allemand I, Riou L, Fouchet P.** Mouse differentiating spermatogonia can generate germinal stem cells *in*

vivo. *Nat Cell Biol* 2009; **11**: 190–196. [Medline] [CrossRef]

32. **Goodell MA, Brose K, Paradis G, Conner AS, Mulligan RC.** Isolation and functional properties of murine hematopoietic stem cells that are replicating *in vivo*. *J Exp Med* 1996; **183**: 1797–1806. [Medline] [CrossRef]

33. **Morita Y, Ema H, Yamazaki S, Nakauchi H.** Non-side-population hematopoietic stem cells in mouse bone marrow. *Blood* 2006; **108**: 2850–2856. [Medline] [CrossRef]

34. **Lo KC, Brugh VM III, Parker M, Lamb DJ.** Isolation and enrichment of murine spermatogonial stem cells using rhodamine 123 mitochondrial dye. *Biol Reprod* 2005; **72**: 767–771. [Medline] [CrossRef]

35. **Shinohara T, Avarbock MR, Brinster RL.** β1- and α6-integrin are surface markers on mouse spermatogonial stem cells. *Proc Natl Acad Sci USA* 1999; **96**: 5504–5509. [Medline] [CrossRef]

36. **Shinohara T, Avarbock MR, Brinster RL.** Functional analysis of spermatogonial stem cells in Steel and cryptorchid infertile mouse models. *Dev Biol* 2000; **220**: 401–411. [Medline] [CrossRef]

37. **Yamaguchi M, Ikebuchi K, Hirayama F, Sato N, Mogi Y, Ohkawara J, Yoshikawa Y, Sawada K, Koike T, Sekiguchi S.** Different adhesive characteristics and VLA-4 expression of $CD34^+$ progenitors in G_0/G_1 versus $S+G_2/M$ phases of the cell cycle. *Blood* 1998; **92**: 842–848. [Medline]

38. **Zaidel-Bar R, Itzkovitz S, Ma'ayan A, Iyengar R, Geiger B.** Functional atlas of the integrin adhesome. *Nat Cell Biol* 2007; **9**: 858–867. [Medline] [CrossRef]

39. **Legate KR, Fässler R.** Mechanisms that regulate adaptor binding to β-integrin cytoplasmic tails. *J Cell Sci* 2009; **122**: 187–198. [Medline] [CrossRef]

40. **Na J, Marsden M, DeSimone DW.** Differential regulation of cell adhesive functions by integrin α subunit cytoplasmic tails *in vivo*. *J Cell Sci* 2003; **116**: 2333–2343. [Medline] [CrossRef]

41. **Kanatsu-Shinohara M, Inoue K, Takashima S, Takehashi M, Ogonuki N, Morimoto H, Nagasawa T, Ogura A, Shinohara T.** Reconstitution of mouse spermatogonial stem cell niches in culture. *Cell Stem Cell* 2012; **11**: 567–578. [Medline] [CrossRef]

42. **Dovere L, Fera S, Grasso M, Lamberti D, Gargioli C, Muciaccia B, Lustri AM, Stefanini M, Vicini E.** The niche-derived glial cell line-derived neurotrophic factor (GDNF) induces migration of mouse spermatogonial stem/progenitor cells. *PLoS One* 2013; **8**: e59431. [Medline] [CrossRef]

43. **Tadokoro Y, Yomogida K, Ohta H, Tohda A, Nishimune Y.** Homeostatic regulation of germinal stem cell proliferation by the GDNF/FSH pathway. *Mech Dev* 2002; **113**: 29–39. [Medline] [CrossRef]

44. **Nagai R, Shinomura M, Kishi K, Aiyama Y, Harikae K, Sato T, Kanai-Azuma M, Kurohmaru M, Tsunekawa N, Kanai Y.** Dynamics of GFRα1-positive spermatogonia at the early stages of colonization in the recipient testes of W/Wᵛ male mice. *Dev Dyn* 2012; **241**: 1374–1384. [Medline] [CrossRef]

45. **de Rooij DG, Lok D, Weenk D.** Feedback regulation of the proliferation of the undifferentiated spermatogonia in the Chinese hamster by the differentiating spermatogonia. *Cell Tissue Kinet* 1985; **18**: 71–81. [Medline]

46. **De Rooij DG, van Dissel-Emiliani FM, van Pelt AM.** Regulation of spermatogonial proliferation. *Ann NY Acad Sci* 1989; **564**: 140–153. [Medline] [CrossRef]

47. **Parreira GG, Ogawa T, Avarbock MR, França LR, Brinster RL, Russell LD.** Development of germ cell transplants in mice. *Biol Reprod* 1998; **59**: 1360–1370. [Medline] [CrossRef]

48. **Simon L, Ekman GC, Garcia T, Carnes K, Zhang Z, Murphy T, Murphy KM, Hess RA, Cooke PS, Hofmann MC.** ETV5 regulates sertoli cell chemokines involved in mouse stem/progenitor spermatogonia maintenance. *Stem Cells* 2010; **28**: 1882–1892. [Medline] [CrossRef]

49. **Chen C, Ouyang W, Grigura V, Zhou Q, Carnes K, Lim H, Zhao G-Q, Arber S, Kurpios N, Murphy TL, Cheng AM, Hassell JA, Chandrashekar V, Hofmann MC, Hess RA, Murphy KM.** ERM is required for transcriptional control of the spermatogonial stem cell niche. *Nature* 2005; **436**: 1030–1034. [Medline] [CrossRef]